ORIGINAL ARTICLE

Modulation of movement-related oscillatory signatures by cognitive interference in healthy aging

Yasra Arif [ORCID] · **Jake J. Son** · **Hannah J. Okelberry** ·
Hallie J. Johnson · **Madelyn P. Willett** ·
Alex I. Wiesman · **Tony W. Wilson**

Abstract Age-related changes in the neurophysiology underlying motor control are well documented, but whether these changes are specific to motor function or more broadly reflect age-related alterations in fronto-parietal circuitry serving attention and other higher-level processes remains unknown. Herein, we collected high-density magnetoencephalography (MEG) in 72 healthy adults (age 28–63 years) as they completed an adapted version of the multi-source interference task that involved two subtypes of cognitive interference (i.e., flanker and Simon) and their integration (i.e., multi-source). All MEG data were examined for age-related changes in neural oscillatory activity using a whole-brain beamforming approach. Our primary findings indicated robust behavioral differences in task performance based on the type of interference, as well as stronger beta oscillations with increasing age in the right dorsolateral prefrontal cortices (flanker and multi-source conditions), left parietal (flanker and Simon), and medial parietal regions (multi-source). Overall, these data indicate that healthy aging is associated with alterations in higher-order association cortices that are critical for attention and motor control in the context of cognitive interference.

Keywords Magnetoencephalography · Multi-source interference task · Motor control · Superadditivity

Y. Arif (✉) · J. J. Son · H. J. Okelberry · H. J. Johnson · M. P. Willett · T. W. Wilson
Institute for Human Neuroscience, Boys Town National Research Hospital, Omaha, NE 68010, USA
e-mail: yasra.arif@boystown.org

J. J. Son
College of Medicine, University of Nebraska Medical Center (UNMC), Omaha, NE, USA

A. I. Wiesman
Montreal Neurological Institute, McGill University, Montreal, QC, Canada

T. W. Wilson
Department of Pharmacology & Neuroscience, Creighton University, Omaha, NE, USA

Introduction

Motor control relies on proper movement planning and execution, which is frequently computed in the context of cognitive interference. While the motor dynamics underlying such processes have been shown to undergo continuous modulation in the primary motor cortex [1–4], there is substantial evidence that fronto-parietal recruitment is even more crucial in the context of interference [4–6]. Specifically, neuronal engagement in the fronto-parietal cortices is thought to form a key element of the preparatory and executory phases of motor function, as the region can exert downstream effects to suppress irrelevant inputs in

the primary and supplementary motor cortices given its additional spatial representations and the visuomotor transformations carried out in the parietal lobes [5, 7–11].

A handful of magnetoencephalographic (MEG) studies have characterized the spectral and temporal parameters of the neural oscillations serving motor control. These studies have revealed strong decreases in the beta rhythm, termed event-related desynchronizations (ERD), shortly before and during movement, which are thought to index motor planning and selection [12–16], 2014). There are also transient increases in gamma activity that coincide with the onset of movement and are generally termed, movement-related gamma synchronizations (MRGS; [1–3, 15, 17–19]. Finally, following movement termination, there is a robust increase in beta activity, termed the post-movement beta rebound (PMBR), which is thought to reflect sensory feedback on the parameters of the completed movement [20–24]. Several recent studies have examined how the abovementioned neural responses are impacted by different forms of cognitive interference in healthy young adults [1, 17, 25]. One recent study by Wiesman and colleagues found that movement-related oscillatory dynamics were affected equally by different subtypes of interference, and that regions of the contralateral premotor cortices exhibited altered MRGS responses during superadditive interference trials (i.e., stimulus-stimulus and stimulus–response; [4, 26, 27].

Though the neurophysiology of cognitive motor control continues to change throughout the adult lifespan [28–30], very little is known about whether the increased susceptibility to interference that comes with aging extends to motor control and the underlying movement-related oscillatory dynamics. Importantly, in a previous aging study, we found increased neural activity in the motor cortices of older participants compared to their younger counterparts, when engaged in a Flanker, stimulus-stimulus interference task [2, 3]. Such additional neural recruitment may indicate age-related compensatory mechanisms, which have been formally described in the compensation-related utilization of neural resources hypothesis (i.e., CRUNCH; [31] and frequently reported in the aging neuroscience literature [32–36]. While the study by Spooner and colleagues provided valuable insights into how motor-related neural signatures are modulated by cognitive interference in healthy aging

adults, it was limited to only one subtype (i.e., stimulus-stimulus interference or the "flanker effect") and the effects were only examined in the motor cortices. Importantly, other subtypes including Simon interference or concurrent presentation of both flanker and Simon (i.e., multi-source) are known to have accentuated effects in the aging population [37–39], but surprisingly almost no work to date has evaluated whether these other subtypes also affect the oscillatory dynamics serving motor control.

In the present study, we collected high-density MEG data in 72 healthy participants (age range 28–63 years) who completed an adaptation of the multi-source-interference task [4, 40, 41] to examine how motor oscillatory signatures are affected by different cognitive interference subtypes in healthy aging. We also aimed to characterize the possibility of convergent, divergent, and superadditive effects of interference subtypes on movement-related responses. In accordance with the literature, we hypothesized age-related compensatory recruitment of neuronal pools mainly within not only fronto-parietal cortices, but also motor-specific regions [2, 3]. We further hypothesized spatially distinct responses based on different interference subtypes, with the flanker effect (i.e., stimulus-stimulus interference) mostly discernable in frontal regions and the Simon effect (i.e., stimulus–response) interference in the parietal cortices [42, 43].

Methods

It should be noted that this study is a comprehensive re-analysis of data reported in a previous study [44]. Importantly, the neural analyses differ substantially from the previous study and do not overlap. The current study examined the effects of cognitive interference on the neural activity locked to the movement onset, as opposed to the visual stimulus that was the focus of the previous study.

Participants

Seventy-two healthy adults (14 females, six left-handed) with a mean age of 50.33 years (range 28–63 years) were enrolled in this study. Histogram for age can be found in the supplementary material (Fig. S1). Exclusionary criteria included

any medical illness affecting CNS function (e.g., HIV/AIDS, lupus), any neurological or psychiatric disorder, history of head trauma, current substance use, and the MEG laboratory's standard exclusion criteria (e.g., ferromagnetic implants). All experimental procedures conformed to the standards set by the *Declaration of Helsinki*. The study protocol was approved by the local Institutional Review Board (IRB). A full description of the study was given to all participants, followed by written informed consent, adhering to the IRB guidelines.

MEG experimental paradigm

A modified version of the multi-source interference task (MSIT; [4, 40, 41, 45, 46] was used to assess cognitive interference effects (Fig. 1 A). Each trial began with a central fixation presented for a randomly varied interstimulus interval of 2000–2400 ms. The fixation was then replaced by a vertically centered horizontal row of three equally spaced integers between 0 and 3. These integer stimuli were presented for 1500 ms. Two of these numbers were always identical (task-irrelevant) and the third was different (task-relevant). Prior to beginning the experiment, participants were given a right-handed five-finger button
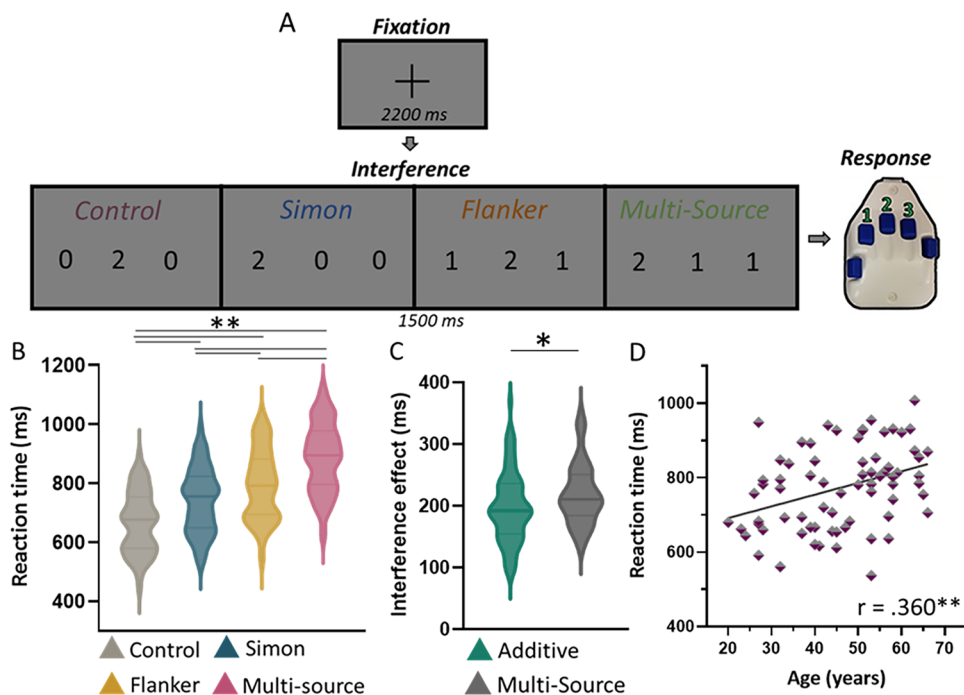
Fig. 1 Experimental paradigm and behavioral performance. (**A**) Each trial began with a central fixation presented for a randomly varied interstimulus interval of 2000–2400 ms. The fixation was then replaced by a vertically centered horizontal row of three equally spaced integers between 0 and 3. The presentation of the integer stimuli lasted for 1500 ms. Two of these integers were always identical (task irrelevant) and the third was different (task relevant). Prior to beginning the experiment, participants were given a five-finger button pad and instructed that the index, middle, and ring finger locations represented the integers 1, 2, and 3, respectively. Participants were then instructed that on each trial they would be presented with a horizontal row of three integers, and that the objective was to indicate the "odd-number-out" by pressing the button corre-sponding to its numerical identity (and not its spatial location). Using these stimuli, four interference conditions were possible: (1) control (no interference), (2) Simon (stimulus–response interference), (3) flanker (stimulus–stimulus interference), and (4) multi-source. (**B**) Results from the behavioral analyses showed a main effect of interference condition, with each condition differing in a stair-step pattern. Reaction time is displayed on the y-axis with interference conditions on the x-axis. (**C**) Behavioral results from the superadditivity model, with reaction time on y-axis and inference conditions (i.e., multi-source and additive effect) on the x-axis. (D) The scatterplot denotes the positive association between chronological age (in years) on the *x*-axis and reaction time collapsed across all four conditions on the y-axis. $*p = 0.05$, $**p = /< 0.001$

pad and instructed that the index, middle, and ring finger locations represented the integers 1, 2, and 3, respectively. Participants were then instructed that on each trial, they would be presented with a horizontal row of three integers and that the objective was to indicate the "odd number-out" by pressing the button corresponding to its numerical identity (and *not* its spatial location). Speed and accuracy were also stressed to the participant at this point. Using these stimuli, four interference conditions were possible: (1) control (no interference; i.e., 1 0 0/0 2 0/0 0 3); (2) Simon (stimulus–response interference; i.e., 0 1 0/0 0 1/2 0 0/0 0 2/0 3 0/3 0 0); (3) Flanker (stimulus–stimulus interference; i.e., 1 2 2/1 3 3/1 2 1/3 2 3/1 1 3/2 2 3); and (4) multi-source (both stimulus–response and stimulus–stimulus interference; i.e., 2 1 2/3 1 3/2 2 1/3 3 1/2 1 1/2 3 3/1 1 2/3 2/1 3 1/2 3 2/3 1 1/3 2 2). Trial types and responses were pseudorandomized over the course of the experiment, such that no interference condition nor any response was repeated more than twice in a row. Participants completed 100 trials of each interference condition, for a grand total of 400 trials, and a total recording time of ~24 min. Custom visual stimuli were programmed in MatLab (Mathworks, Inc.) using the Psychophysics Toolbox Version 3 [47] and back-projected onto a nonmagnetic screen.

MEG data acquisition

All recordings were conducted in a one-layer magnetically shielded room with active shielding engaged for environmental noise compensation. With an acquisition bandwidth of 0.1–330 Hz, neuromagnetic responses were sampled continuously at 1 kHz using a MEGIN MEG system (Helsinki, Finland) with 306 sensors, including 204 planar gradiometers and 102 magnetometers. During data acquisition, participants were monitored via real-time audio-visual feeds from inside the shielded room. Each MEG dataset was individually corrected for head motion and subjected to noise reduction using the signal space separation method with a temporal extension [48].

Structural MRI processing and MEG co-registration

Prior to MEG measurement, four coils were attached to the subject's head and localized, together with the three fiducial points and scalp surface, with a 3-D digitizer (FASTRAK 3SF0002, Polhemus Navigator Sciences, Colchester, VT, USA). Once the subjects were positioned for MEG recording, an electric current with a unique frequency label (e.g., 322 Hz) was fed to each of the coils. This induced a measurable magnetic field and allowed each coil to be localized in reference to the sensors throughout the recording session. As coil locations were also known with respect to head coordinates, all MEG measurements could be transformed into a common coordinate system. With this coordinate system, each participant's MEG data were co-registered with their T1-weighted structural MRI prior to source space analysis using BESA MRI (Version 2.0). Structural T1-weighted MRI images were acquired using a Siemens Prisma 3-Tesla MRI scanner with a 64-channel head coil and an MP-RAGE sequence with the following parameters: TR = 2300 ms; TE = 2.98 ms; flip angle = 9°; FOV = 256 mm; slice thickness = 1 mm (no gap); voxel size = $1 \times 1 \times 1$ mm. These data were aligned parallel to the anterior and posterior commissures and transformed into standardized space. Following source analysis (i.e., beamforming), each subject's functional MEG images were also transformed into standardized space using the transform that was previously applied to the structural MRI volume and spatially resampled.

MEG preprocessing, time–frequency transformation, and sensor-level statistics

Eye blinks and cardiac artifacts were removed from the data using signal space projection (SSP), which was accounted for during source reconstruction [49]. The continuous magnetic time series was then divided into 3500 ms epochs, with movement onset as time 0 and the baseline extending from –1600 to –1100 ms prior to movement (i.e., button press). Epochs containing artifacts were removed based on a fixed threshold method, and supplemented with visual inspection. In brief, for each individual, the distributions of amplitude and gradient values across all trials were computed, and those trials containing the highest amplitude and/or gradient values relative to the full distribution were rejected by selecting a threshold that excluded extreme values. Importantly, these thresholds were set individually for each participant, as inter-individual differences in variables such as head size and proximity to the sensors strongly

affect MEG signal amplitude. An average amplitude threshold of 1282.29 (SD = 263.47) fT/cm and an average gradient threshold of 263.47 (SD = 124.78) fT/(cm*ms) were used to reject artifacts. Across the group, an average of 362 (SD = 22) trials per participant were used for further analysis. To ensure there were no systematic differences in the number of trials per participant, an ANCOVA was run, and this showed no significant main effect of condition, age, or the interaction, all p's > 0.05.

Artifact-free epochs were transformed into the time–frequency domain using complex demodulation [50], with a time/frequency resolution of 2 Hz/25 ms and a bandwidth of 4–100 Hz. The resulting spectral power estimations per sensor were averaged across trials to generate a mean time series per sensor. These sensor-level data were normalized per time–frequency bin using the respective bin's baseline power, which was calculated as the mean power during the −1600 to −1100 ms baseline period. The specific time–frequency windows used for source reconstruction were determined by statistical analysis of the sensor-level spectrograms across all participants using the entire array of 204 gradiometers. Briefly, each data point in the spectrogram was initially evaluated using a mass univariate approach based on the general linear model. To reduce the risk of false-positive results while maintaining reasonable sensitivity, a two-stage procedure was followed to control for type 1 error. In the first stage, two-tailed paired-sample t-tests against baseline were conducted on each data point, and the output spectrogram of t-values was thresholded at $p < 0.001$ to define time–frequency bins containing potentially significant oscillatory deviations across all participants. In stage 2, time–frequency bins that survived the threshold were clustered with temporally and/or spectrally neighboring bins that were also above the threshold ($p < 0.01$), and a cluster value was derived by summing the t-values of all data points in the cluster. Nonparametric permutation testing was then used to derive a distribution of cluster values, and the significance level of the observed clusters (from stage 1) were tested directly using this distribution [51, 52]. For each comparison, 10,000 permutations were computed. Note that our initial statistical threshold and nonparametric approach to multiple comparisons was based on the recommendations of Eklund et al. [53] and are considered among the most rigorous approaches in human neuroimaging. Based

on these analyses, the time–frequency windows that contained significant oscillatory events across all participants and conditions were subjected to the beamforming analysis. The sensor-level analysis was performed in Brain Electrical Source Analysis (BESA) statistics software 2.0. For further details on our data processing pipeline, see 45, 46.

MEG source imaging and statistics

Oscillatory neural responses were imaged using the dynamic imaging of coherent sources (DICS) beamformer [54], which applies spatial filters in the time–frequency domain to calculate voxel-wise source power for the entire brain volume. The single images were derived from the cross-spectral densities of all combinations of MEG gradiometers averaged over the time–frequency range of interest and the solution of the forward problem for each location on a grid specified by input voxel space. Following convention, we computed noise-normalized source power for each voxel per participant using active (i.e., task) and passive (i.e., baseline) periods of equal duration and bandwidth [55] at a resolution of $4.0 \times 4.0 \times 4.0$ mm. Such images are typically referred to as pseudo-t maps, with units (pseudo-t) that reflect noise-normalized power differences (i.e., active versus passive) per voxel. MEG preprocessing and imaging used the BESA research (V7) software. To assess the neuroanatomical basis of the significant oscillatory responses identified through the sensor-level analysis, mean whole-brain maps were computed across all interference conditions and participants for the selected time–frequency windows.

To evaluate age-dependent interference-related differences in oscillatory power, we performed a voxelwise subtraction of the control condition from each of the three interference conditions for each participant per time–frequency component. This resulted in participant-level whole-brain subtraction maps for each of the Simon, flanker, and multi-source interference conditions. Additionally, to investigate the potential for superadditivity of multi-source interference on neural activity, the voxel-wise power values of the Simon and flanker interference maps were summed to produce a whole-brain map (per participant, per neural response), which was then subtracted from the multi-source map and subjected to whole-brain voxelwise correlation analyses, with age as the covariate of

interest. To control for type I error, maps were thresholded at $p < 0.001$ to define potentially significant clusters and then nonparametric permutation testing was conducted, similar to that performed on the sensor-level spectrograms, with at least 10,000 permutations per comparison. All the correlational analyses were performed in BESA statistics (2.0). Following which, Bayesian testing was conducted on all our findings which indicated evidence for the alternative hypothesis.

Results

Behavioral performance

Repeated-measures ANCOVA on the behavioral data revealed significant effects of interference condition on reaction time (RT), $F_{(3,69)} = 47.18$, $p < 0.001$, and age, $F_{(1,69)} = 9.32$, $p = 0.003$. Post hoc comparisons showed that participants were significantly slower to respond on the Simon, $t(71) = -19.57$, $p < 0.001$, flanker, $t(71) = -22.18$, $p < 0.001$, and multi-source, $t(71) = -36.68$, $p < 0.001$, conditions compared to the control trials. Furthermore, participants were significantly slower in the multi-source condition than both the Simon, $t(71) = 16.83$, $p < 0.001$, and flanker, $t(71) = 26.42$, $p < 0.001$, conditions and responded significantly slower on flanker than Simon trials, $t(71) = 9.58$, $p < 0.001$ (Fig. 1 B). Additionally, reaction time increased significantly with advancing age across all conditions, $r = 0.360$, $p = 0.001$ (Fig. 1 C), and the age-by-condition interaction effect was not significant, $F_{(3, 74)} = 2.57$, $p = 0.080$. To probe potential age-related superadditivity effects on MSIT performance, a 1×2 ANCOVA comparing the effects of multi-source interference and the additive model (Simon interference + flanker interference) was conducted, which showed a significant main effect of condition for RT, $F_{(1, 70)} = 4.28$, $p = 0.042$, such that the concurrent presentation of the two interference sources (i.e., multi-source condition) worsened behavior, as compared to the additive effects of Simon and flanker interference in isolation (Fig. 1 D). Post hoc were corrected using Holm's method. Finally, neither the main effect of age $F_{(1, 70)} = 0.36$, $p = 0.553$, nor the interaction $F_{(1, 70)} = 0.29$, $p = 0.589$, was significant for the superadditivity reaction time

effect. Finally, no main effects or interactions with accuracy were found, all p's > 0.100.

MEG sensor and source-level oscillatory analysis

After transforming the data into time–frequency space, we observed robust activity in the beta and gamma bands in sensors near the sensorimotor cortices (Fig. 2). Specifically, a significant decrease or desynchronization was observed in the beta band (16–26 Hz; −400 to 100 ms, $p < 0.001$, corrected), while a strong increase from baseline or synchronization was seen in the gamma band (68–76 Hz; −50 to 100 ms, $p < 0.001$, corrected) The time–frequency windows of interest were then imaged using a beamformer and the resulting maps per response were averaged over all participants and conditions. Source imaging of these time–frequency windows revealed that the beta and gamma responses were originating from the hand-knob region of the precentral gyrus, suggesting these responses likely reflect the motor components of the behavioral response. Finally, we did not image the PMBR response, as it was after movement offset and the condition-wise reaction time differences would potentially confound any significant findings.

Age-related conditional differences on beta and gamma oscillatory responses

To examine the impact of aging on neural oscillatory activity serving movement during the three types of cognitive interference, interference effect maps were computed by subtracting the control condition power map from each conditional map and then performing voxel-wise correlations with age. For flanker interference, an increase in beta oscillatory response strength (i.e., more negative) with increasing age was observed in the right dorsolateral prefrontal cortex ($r = -0.487$, $p_{corr} = 0.005$, $p_{uncorr} < 0.0005$, $BF_{10} = 316.26$), left inferior parietal ($r = -0.528$, $p_{corr} = 0.014$, $p_{uncorr} = 0.0005$, $BF_{10} = 1846.09$), and right parietal ($r = -0.457$, $p_{corr} = 0.037$, $p_{uncorr} < 0.0005$, $BF_{10} = 126.93$; Fig. 3). Similarly, for Simon interference, stronger beta oscillations (i.e., more negative) with increasing age were found in the bilateral parietal cortices (L: $r = -0.472$, $p_{corr} = 0.065$, $p_{uncorr} < 0.0005$, $BF_{10} = 212.81$; R: $r = -0.457$, $p_{corr} = 0.084$,
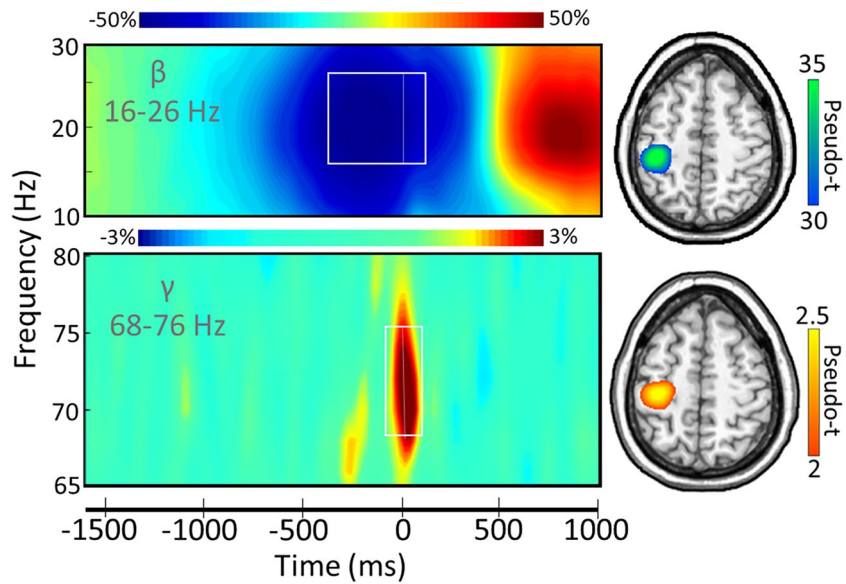
Fig. 2 Sensor-level time–frequency analysis. The MEG sensor spectrograms (left) display the time–frequency representations of neural responses identified by cluster-based permutation analysis (see "Methods" section), highlighted using the white dotted boundaries. Time (in ms) is denoted on the *x*-axis and frequency (in Hz) on the *y*-axis, with the dashed white line at 0 ms indicating the motor response. The color scale bar for percent change from baseline is displayed above each plot. Each spectrogram represents group- and condition-averaged data from one gradiometer sensor that was representative of the neural response in sensors near somato-motor regions. On the far right is the source-imaged representation of each response (beta ERD and MRGS), grand-averaged across all conditions and participants, with the color scale bar to the right denoting response amplitude in pseudo-*t* units
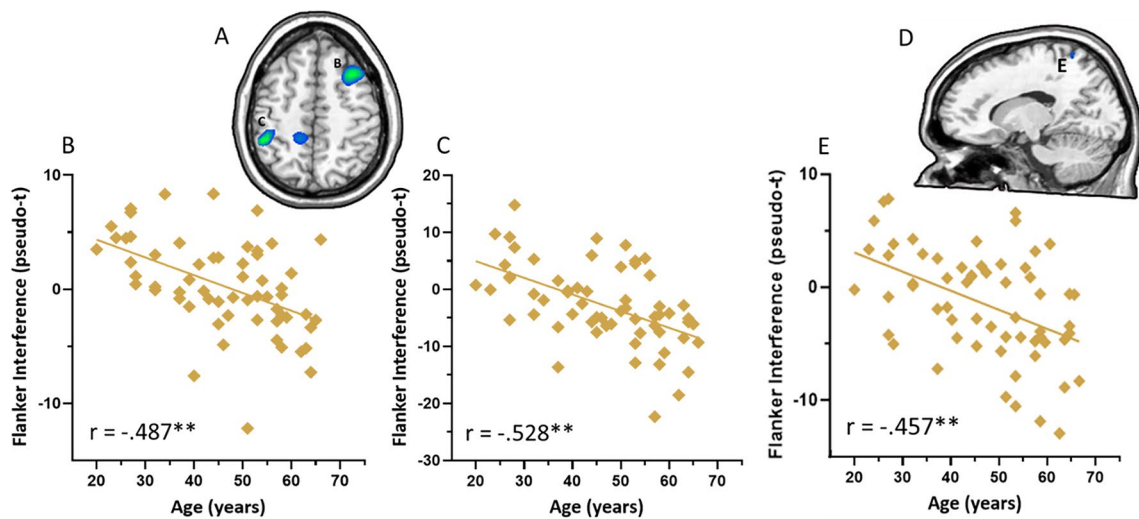
Fig. 3 Effects of aging on flanker interference: Whole-brain voxel-wise correlational analysis of flanker interference maps with age revealed stronger beta oscillations (i.e., more negative) in (**B**) the right dorsolateral prefrontal cortex, (**C**) left parietal, and (**E**) right parietal. ** $p < 0.001$, uncorrected

Fig. 4 Effects of aging on Simon interference: Whole-brain voxel-wise correlational analysis of Simon interference maps with age revealed stronger beta oscillations with increasing age in the (**A**, **B**) left, and (**C**, **D**) right parietal cortices. ** $p < 0.001$, uncorrected
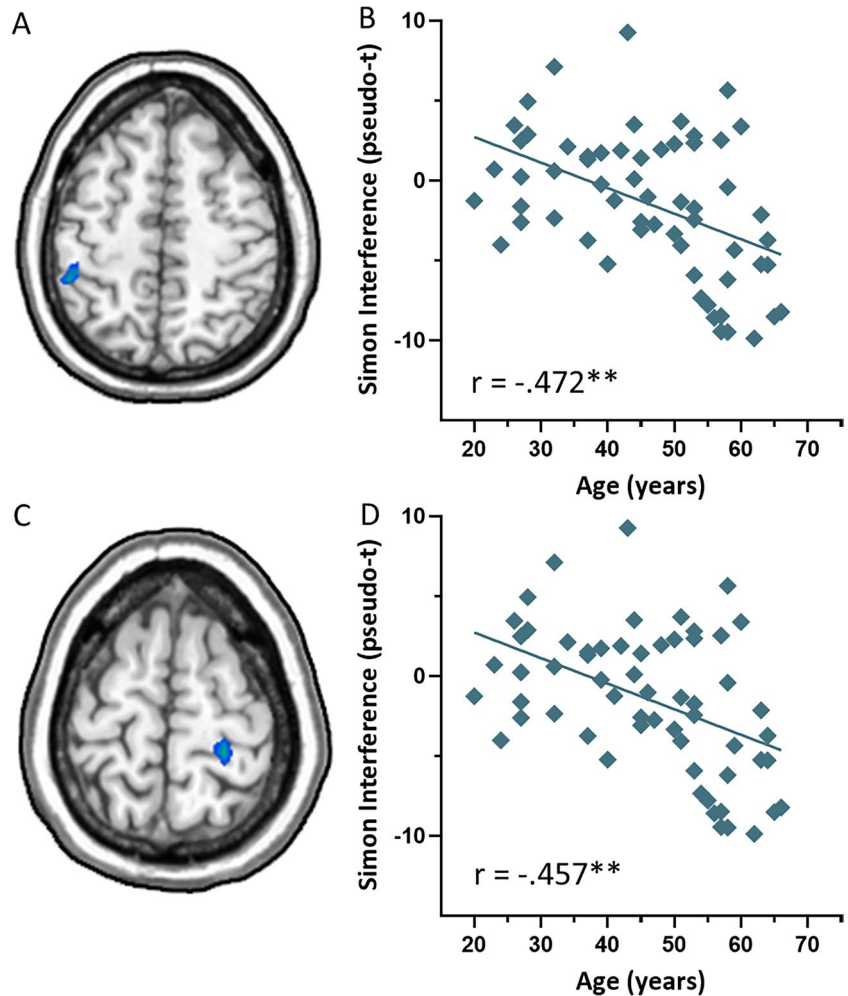
$p_{uncorr} < 0.0005$, $BF_{10} = 115.11$; Fig. 4). Similar results were found for the multi-source condition, with stronger beta oscillations with increasing age in the right dorsolateral prefrontal, $r = -0.456$, $p_{corr} = 0.07$, $p_{uncorr} < 0.0005$, $BF_{10} = 110.71$, and left medial parietal cortices, $r = -0.526$, $p_{corr} = 0.02$, $p_{uncorr} < 0.0005$, $BF_{10} = 1433.15$ (Fig. 5 A, B).

Finally, we examined the superadditivity effect by subtracting the additive model (flanker + Simon interference) from the multi-source interference condition and correlating the output with age. This revealed that the stronger beta oscillations during the multi-source condition became weaker in the right DLPFC with increasing age, $r = 0.419$, $p_{corr} = 0.059$, $p_{uncorr} < 0.0005$, $BF_{10} = 36.77$ (Fig. 6). Lastly, for the gamma band, the only significant age correlation was observed in the left cerebellum during the flanker

condition, $r = -0.483$, $p_{corr} = 0.067$, $p_{uncorr} < 0.0005$, $BF_{10} = 362.22$.

Discussion

In this study, we used an adaptation of the MSIT paradigm [4] and whole-brain statistical analyses to characterize how healthy aging impacts neural dynamics serving motor planning and execution in the face of distinct cognitive distractors. Behavioral performance reflected progressively increasing difficulty of the interference conditions from control to Simon, flanker, and then multi-source, while aging showed an overall decline (i.e., increased reaction time) irrespective of the interference condition. Meanwhile, the neural oscillations serving motor control were
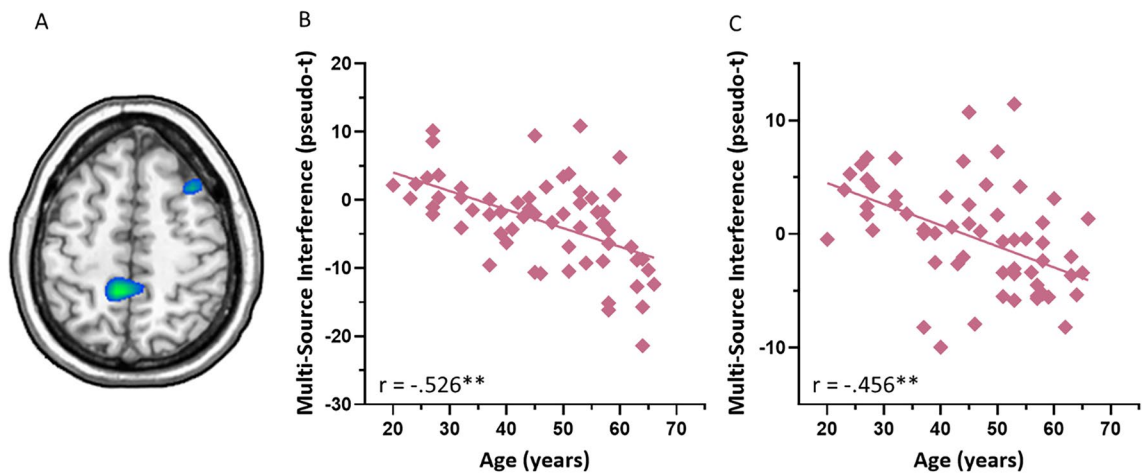
Fig. 5 Effects of aging on multi-source interference and superadditivity model: Whole-brain voxel-wise correlational analysis of multi-source interference maps with age revealed stronger beta oscillations power in (**A**) left medial parietal and (**B**) right dorsolateral prefrontal cortices. **$p < 0.001$, uncorrected

Fig. 6 Superadditivity effects: Whole-brain voxel-wise correlational analysis of the superadditivity model showed decreases in the stronger beta oscillations during multi-source interference with increasing age in the right dorsolateral prefrontal cortices. **$p < 0.001$, uncorrected
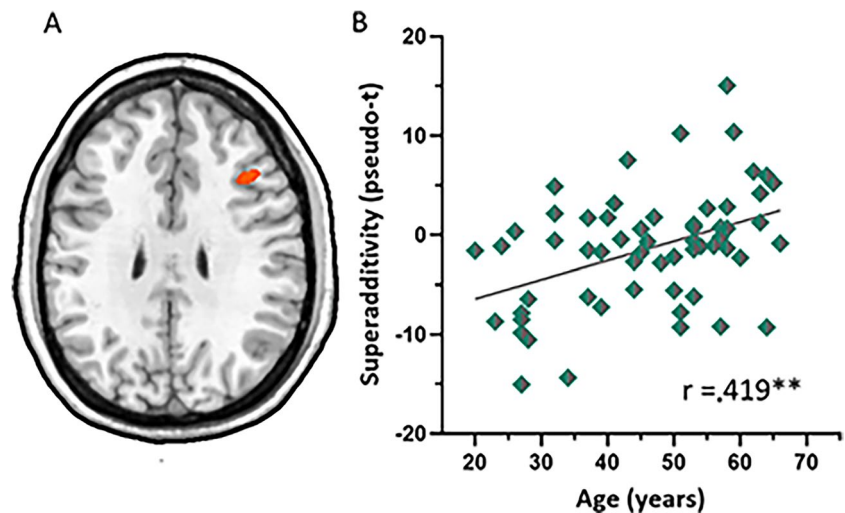
modulated by aging in an interference subtype-specific way, which suggests that the aging brain adapts differential patterns of neural responses based on the nature of interference. Stronger beta interference effects with increasing age were observed in the right DLPFC (flanker and multi-source), left parietal (flanker and Simon), medial parietal (multi-source), and other brain regions. Interestingly, the superadditivity model suggested that the stronger beta response in the right DLPFC during multi-source interference was becoming weaker with increasing age. Finally, in contrast to beta, age-sensitive gamma interference effects were found only in the cerebellum and

limited to flanker-type interference. Below, we discuss the implications of these novel findings to better understand interference-related changes in the neural dynamics serving motor control in the aging population.

As mentioned earlier, higher-order inputs are critical in resolving cognitive conflicts. For example, flanker interference prompts selective attention processing to suppress inappropriate responses by inducing inhibitory signals from the prefrontal and parietal cortices [42, 56–58]. Likewise, Simon interference, where there is a spatial incompatibility between stimulus and response location, is conditional not only on

the top-down feedback but also on continual updating of the spatial representation by the parietal cortices for successful task execution [59]. Importantly, it has been recently reported that similar top-down executive control is required to modulate movement-related oscillations in the motor system in response to cognitive interference [4]. Our findings not only support previous reports, but also delineate how these neural signatures of motor control are impacted by healthy aging. Broadly, significant age-related increases in beta neural response power (i.e., more desynchronization) that were observed in the presence of cognitive interference suggest compensatory recruitment of interference-subtype–dependent cortical regions to meet the increasing demands of the task. However, interestingly, our data also suggest that such neural hyperactivity with aging does not directly translate into improved behavioral performance. This may indicate the exhaustion of such compensatory strategies or that other parts of the output system also experience some form of aging-related cost (e.g., muscular/non-neural). The prefrontal cortices are considered most vulnerable to the effects of aging with a collection of studies reporting cortical thinning [60], gray matter atrophy, and volume reduction in these regions in older participants [61, 62]. Similar changes have also been shown in the parietal lobes with advancing age [63, 64].

Importantly, an alternative interpretation for such age-related cortical hyperactivity during interference could also be tied to the dedifferentiation theory of aging [65], which postulates non-selective engagement of neuronal pools and thus neural inefficiency secondary to neuromodulatory changes with age [66–68]. Future investigations using multi-modal approaches may help elucidate the complex interplay between altered neurotransmission, reduction in neural selectivity, and cortical hyper-activity with increasing age.

Surprisingly, the beta superadditive effects were found to decrease with age in the right DLPFC, which is probably suggestive of age-related convergence of neural resource allocation when two interference models with higher cognitive loads (i.e., Simon and flanker subtypes presented in tandem versus individually) are juxtaposed. Contrasting this pattern of neural activity in the right DLPFC with our previous findings of age-related increase in DLPFC beta power in the case of flanker interference alone may suggest

neural resource depletion, such that the cumulative interference load may have exceeded the processing capacity for interference resolution with aging thus manifesting "cognitive fatigue" [69]. Moreover, our superadditive effects can be tied to "the processing speed theory of adult age" [70], with cognitive overload further impacting processing speed with advancing age, reflected in decreased DLPFC recruitment during multisource as compared to additive interference [71]. Lastly, in contrast to the beta findings, weaker gamma interference effects with age were elicited by the flanker subtype in the left cerebellum. The contribution of cerebellar circuitry in motor control has been highlighted by multiple studies in both health and disease [72, 73]. Additionally, an fMRI study posited changes in the connectivity of the cerebellum with frontal and motor cortices during response inhibition [74]. Further support for cerebellar-cerebral interactions during inhibitory control comes from brain stimulation studies where anodal transcranial direct current stimulation (tDCS of the cerebellum resulted in potentiated cerebellar brain inhibition (i.e., CBI: pathway extending between the cerebellum and motor cortices; [75], whereas a later study suggested CBI reduction following cathodal tDCS of the cerebellum [76]. Taken together with the loss of Purkinje cells in the cerebellum reported by both animal and human studies with aging [77, 78], our gamma finding may indicate age-related deficits in inhibitory control and thus impaired response inhibition.

Before closing, it is important to acknowledge several limitations of the current work. First, our most robust age-related findings were in the flanker interference condition, which survived our stringent nonparametric permutation testing approach to control for type 1 error. This could reflect that flanker type interference is most susceptible to aging effects [79], but future studies are needed to confirm this. Second, not all of the age-related Simon and multisource neural interference effects survived correction with nonparametric permutation testing. While the Bayes factors for all of these comparisons were large and suggested strong or extremely strong evidence for the alternative hypothesis, these findings should still be interpreted with caution. Similar caveats apply to the age-related superadditivity effects that we reported here. Finally, there are known limitations with using cross-sectional approaches in the context of aging

and developmental studies and these limitations apply to the current work and must be kept in mind when interpreting and generalizing our age-related findings.

To close, our findings indicate that the impact of cognitive interference on the cortical dynamics serving motor control is subtype specific and involves higher order frontal and parietal cortices. Overall, our data corroborate prior literature by implicating age-related alterations in the top-down control of movement and provide novel insight into how differential brain regions and neural response patterns are leveraged to overcome cognitive interference subtypes with advancing age. Future studies should investigate potential changes in functional connectivity with increasing age in the regions indicated in this study. Importantly, along with conventional computation of motor beta response (i.e., spectral averaging approach), emerging literature has provided mechanistic insight into the functional role of transient high-power "burst-like" events during motor task performance, with their different parameters (i.e., count, timing, and/or peak event power) predicting behavioral outcomes [2, 3, 80]. Specifically, in the context of aging, it has been suggested that the changes in beta-induced activity observed with increasing age may in part be due to alterations in the cortical burst characteristics embedded within the averaged trials [81]. Future aging studies on movement dynamics could likely help draw parallels between the two approaches and advance our understanding of how trial-to-trial variations in motor responses may contribute to the mean beta power.

Disclaimer

The funders had no role in study design, data collection, and analysis, decision to publish, or preparation of the manuscript.

Declarations

References

1. Heinrichs-Graham E, Hoburg JM, Wilson TW. The peak frequency of motor-related gamma oscillations is modulated by response competition. Neuroimage. 2018;165:27–34. https://doi.org/10.1016/j.neuroimage.2017.09.059.

2. Spooner RK, Arif Y, Taylor BK, Wilson TW. Movement-related gamma synchrony differentially predicts behavior in the presence of visual interference across the lifespan. Cereb Cortex. 2021;31:5056–66.

3. Spooner RK, Taylor BK, Ahmad IM, Dyball KN, Emanuel K, Fox HS, Stauch KL, Zimmerman MC, Wilson TW. Neural oscillatory activity serving sensorimotor control is predicted by superoxide-sensitive mitochondrial redox environments. Proc Natl Acad Sci. 2021;118:e2104569118. https://doi.org/10.1073/pnas.2104569118.

4. Wiesman AI, Koshy SM, Heinrichs-Graham E, Wilson TW. Beta and gamma oscillations index cognitive interference effects across a distributed motor network. Neuroimage. 2020;213:116747. https://doi.org/10.1016/j.neuroimage.2020.116747.

5. Hordacre B, Lotze M, Jenkinson M, Lazari A, Barras CD, Boyd L, Hillier S. Fronto-parietal involvement in chronic stroke motor performance when corticospinal tract integrity is compromised. NeuroImage Clin. 2021;29:102558. https://doi.org/10.1016/j.nicl.2021.102558.

6. Ptak R, Schnider A, Fellrath J. The dorsal frontoparietal network: a core system for emulated action. Trends Cogn Sci. 2017;21:589–99.

7. Convento S, Bolognini N, Fusaro M, Lollo F, Vallar G. Neuromodulation of parietal and motor activity affects motor planning and execution. Cortex. 2014;57:51–9.

8. Hanakawa T, Dimyan MA, Hallett M. Motor planning, imagery, and execution in the distributed motor network: a time-course study with functional MRI. Cereb Cortex. 2008;18:2775–88. https://doi.org/10.1093/cercor/bhn036.

9. Heinrichs-Graham E, Taylor BK, Wang Y-P, Stephen JM, Calhoun VD, Wilson TW. Parietal oscillatory dynamics mediate developmental improvement in motor performance. Cereb Cortex. 2020;30:6405–14.

10. Mountcastle VB, Lynch JC, Georgopoulos A, Sakata H, Acuna C. Posterior parietal association cortex of the monkey: command functions for operations within extrapersonal space. J Neurophysiol. 1975;38:871–908. https://doi.org/10.1152/jn.1975.38.4.871.

11. Thoenissen D, Zilles K, Toni I. Differential involvement of parietal and precentral regions in movement preparation and motor intention. J Neurosci. 2002;22:9024–34.

12. Brovelli A, Ding M, Ledberg A, Chen Y, Nakamura R, Bressler SL. Beta oscillations in a large-scale sensorimotor cortical network: directional influences revealed by Granger causality. Proc Natl Acad Sci. 2004;101:9849–54. https://doi.org/10.1073/pnas.0308538101.

13. Heinrichs-Graham E, Wilson TW. Coding complexity in the human motor circuit. Hum Brain Mapp. 2015;36:5155–67. https://doi.org/10.1002/hbm.23000.

14. Kurz MJ, Becker KM, Heinrichs-Graham E, Wilson TW. Neurophysiological abnormalities in the sensorimotor cortices during the motor planning and movement execution stages of children with cerebral palsy. Dev Med Child Neurol. 2014;56:1072–7. https://doi.org/10.1111/dmcn.12513.

15. Wilson TW, Slason E, Asherin R, Kronberg E, Reite ML, Teale PD, Rojas DC. An extended motor network generates beta and gamma oscillatory perturbations during development. Brain Cogn. 2010;73:75–84. https://doi.org/10.1016/j.bandc.2010.03.001.

16. Wilson TW, Slason E, Asherin R, Kronberg E, Teale PD, Reite ML, Rojas DC. Abnormal gamma and beta MEG activity during finger movements in early-onset psychosis. Dev Neuropsychol. 2011;36:596–613. https://doi.org/10.1080/87565641.2011.555573.

17. Gaetz W, Liu C, Zhu H, Bloy L, Roberts TPL. Evidence for a motor gamma-band network governing response interference. Neuroimage. 2013;74:245–53. https://doi.org/10.1016/j.neuroimage.2013.02.013.

18. Muthukumaraswamy SD. Temporal dynamics of primary motor cortex gamma oscillation amplitude and piper corticomuscular coherence changes during motor control. Exp Brain Res. 2011;212:623–33. https://doi.org/10.1007/s00221-011-2775-z.

19. Muthukumaraswamy SD. Functional properties of human primary motor cortex gamma oscillations. J Neurophysiol. 2010;104:2873–85. https://doi.org/10.1152/jn.00607.2010.

20. Cassim F, Monaca C, Szurhaj W, Bourriez J-L, Defebvre L, Derambure P, Guieu J-D. Does post-movement beta synchronization reflect an idling motor cortex? NeuroReport. 2001;12:3859–63.

21. Fry A, Mullinger KJ, O'Neill GC, Barratt EL, Morris PG, Bauer M, Folland JP, Brookes MJ. Modulation of post-movement beta rebound by contraction force and rate of force development. Hum Brain Mapp. 2016;37:2493–511.

22. Reyns N, Houdayer E, Bourriez JL, Blond S, Derambure P. Post-movement beta synchronization in subjects presenting with sensory deafferentation. Clin Neurophysiol. 2008;119:1335–45.

23. Sallard E, Tallet J, Thut G, Deiber M-P, Barral J. Post-switching beta synchronization reveals concomitant sensory reafferences and active inhibition processes. Behav Brain Res. 2014;271:365–73.

24. Tan H, Wade C, Brown P. Post-movement beta activity in sensorimotor cortex indexes confidence in the estimations from internal models. J Neurosci. 2016;36:1516–28.

25. Grent-'t-Jong T, Oostenveld R, Jensen O, Medendorp WP, Praamstra P. Oscillatory dynamics of response competition in human sensorimotor cortex. NeuroImage. 2013;83:27–34. https://doi.org/10.1016/j.neuroimage.2013.06.051.

26. Eriksen BA, Eriksen CW. Effects of noise letters upon the identification of a target letter in a nonsearch task. Percept Psychophys. 1974;16:143–9. https://doi.org/10.3758/BF03203267.

27. Simon, J.R., 1990. The effects of an irrelevant directional CUE on human information processing, in: Proctor, R.W., Reeve, T.G. (Eds.), Advances in psychology, stimulus-response compatibility. North-Holland, pp. 31–86. https://doi.org/10.1016/S0166-4115(08)61218-2

28. Poirier G, Ohayon A, Juranville A, Mourey F, Gaveau J. Deterioration, compensation and motor control processes in healthy aging, mild cognitive impairment and Alzheimer's disease. Geriatrics. 2021;6:33.

29. Seidler RD, Bernard JA, Burutolu TB, Fling BW, Gordon MT, Gwin JT, Kwak Y, Lipps DB. Motor control and aging: links to age-related brain structural, functional, and biochemical effects. Neurosci Biobehav Rev. 2010;34:721–33.

30. Shaver A (2019) The effects of aging on cognitive motor control

31. Reuter-Lorenz PA, Cappell KA. Neurocognitive aging and the compensation hypothesis. Curr Dir Psychol Sci. 2008;17:177–82. https://doi.org/10.1111/j.1467-8721.2008.00570.x.

32. Arif Y, Spooner RK, Wiesman AI, Embury CM, Proskovec AL, Wilson TW (2020) Modulation of attention networks serving reorientation in healthy aging. Aging 12, 12582–12597. https://doi.org/10.18632/aging.103515

33. Cappell KA, Gmeindl L, Reuter-Lorenz PA. Age differences in prefontal recruitment during verbal working memory maintenance depend on memory load Cortex. Cogn Neurosci Aging. 2010;46:462–73. https://doi.org/10.1016/j.cortex.2009.11.009.

34. Heuninckx S, Wenderoth N, Swinnen SP. Systems neuroplasticity in the aging brain: recruiting additional neural resources for successful motor performance in elderly persons. J Neurosci. 2008;28:91–9.

35. Proskovec AL, Heinrichs-Graham E, Wilson TW. Aging modulates the oscillatory dynamics underlying successful working memory encoding and maintenance. Hum Brain Mapp. 2016;37:2348–61.

36. Schneider-Garces NJ, Gordon BA, Brumback-Peltz CR, Shin E, Lee Y, Sutton BP, Maclin EL, Gratton G, Fabiani M. Span, CRUNCH, and beyond: working memory capacity and the aging brain. J Cogn Neurosci. 2010;22:655–69. https://doi.org/10.1162/jocn.2009.21230.

37. Kawai N, Kubo-Kawai N, Kubo K, Terazawa T, Masataka N. Distinct aging effects for two types of inhibition in older adults: a near-infrared spectroscopy study on the Simon task and the flanker task. NeuroReport. 2012;23:819. https://doi.org/10.1097/WNR.0b013e3283578032.

38. Scrivano RM, Kieffaber PD. Behavioral and electrophysiological correlates of Simon and flanker conflict interference in younger and older adults. Neuropsychol Dev Cogn B Aging Neuropsychol Cogn. 2022;29:318–48. https://doi.org/10.1080/13825585.2021.1874278.

39. Sebastian A, Baldermann C, Feige B, Katzev M, Scheller E, Hellwig B, Lieb K, Weiller C, Tüscher O, Klöppel S. Differential effects of age on subcomponents of response inhibition. Neurobiol Aging. 2013;34:2183–93. https://doi.org/10.1016/j.neurobiolaging.2013.03.013.

40. Bush G, Shin LM. The Multi-Source Interference Task: an fMRI task that reliably activates the

cingulo-frontal-parietal cognitive/attention network. Nat Protoc. 2006;1:308–13. https://doi.org/10.1038/nprot.2006.48.

41. Bush G, Shin LM, Holmes J, Rosen BR, Vogt BA. The Multi-Source Interference Task: validation study with fMRI in individual subjects. Mol Psychiatry. 2003;8:60–70. https://doi.org/10.1038/sj.mp.4001217.

42. Fassbender C, Foxe JJ, Garavan H. Mapping the functional anatomy of task preparation: priming task-appropriate brain networks. Hum Brain Mapp. 2006;27:819–27. https://doi.org/10.1002/hbm.20223.

43. Schiff S, Bardi L, Basso D, Mapelli D. Timing spatial conflict within the parietal cortex: a TMS study. J Cogn Neurosci. 2011;23:3998–4007. https://doi.org/10.1162/jocn_a_00080.

44. Arif Y, Wiesman AI, Christopher-Hayes N, Okelberry HJ, Johnson HJ, Willett MP, Wilson TW. Altered age-related alpha and gamma prefrontal-occipital connectivity serving distinct cognitive interference variants. Neuroimage. 2023;280:120351. https://doi.org/10.1016/j.neuroimage.2023.120351.

45. Wiesman AI, Wilson TW. Posterior alpha and gamma oscillations index divergent and superadditive effects of cognitive interference. Cereb Cortex. 2020;30:1931–45. https://doi.org/10.1093/cercor/bhz214.

46. Wiesman AI, Wilson TW. Attention modulates the gating of primary somatosensory oscillations. Neuroimage. 2020;211:116610.

47. Brainard DH, Vision S. The psychophysics toolbox. Spat Vis. 1997;10:433–6.

48. Taulu S, Simola J. Spatiotemporal signal space separation method for rejecting nearby interference in MEG measurements. Phys Med Biol. 2006;51:1759.

49. Uusitalo MA, Ilmoniemi RJ. Signal-space projection method for separating MEG or EEG into components. Med Biol Eng Comput. 1997;35:135–40.

50. Hoechstetter K, Bornfleth H, Weckesser D, Ille N, Berg P, Scherg M. BESA source coherence: a new method to study cortical oscillatory coupling. Brain Topogr. 2004;16:233–8.

51. Ernst MD (2004) Permutation methods: a basis for exact inference. Stat Sci 676–685

52. Maris E, Oostenveld R. Nonparametric statistical testing of EEG-and MEG-data. J Neurosci Methods. 2007;164:177–90.

53. Eklund A, Nichols TE, Knutsson H. Cluster failure: why fMRI inferences for spatial extent have inflated false-positive rates. Proc Natl Acad Sci. 2016;113:7900–5. https://doi.org/10.1073/pnas.1602413113.

54. Gross J, Kujala J, Hämäläinen M, Timmermann L, Schnitzler A, Salmelin R. Dynamic imaging of coherent sources: studying neural interactions in the human brain. Proc Natl Acad Sci. 2001;98:694–9.

55. Hillebrand A, Singh KD, Holliday IE, Furlong PL, Barnes GR. A new approach to neuroimaging with magnetoencephalography. Hum Brain Mapp. 2005;25:199–211.

56. Chen T, Wang H, Wang X, Zhu C, Zhang L, Wang K, Yu F. Transcranial direct current stimulation of the right dorsolateral prefrontal cortex improves response inhibition. Int J Psychophysiol Off J Int Organ Psychophysiol.

2021;162:34–9. https://doi.org/10.1016/j.ijpsycho.2021.01.014.

57. Spooner RK, Eastman JA, Rezich MT, Wilson TW. High-definition transcranial direct current stimulation dissociates fronto-visual theta lateralization during visual selective attention. J Physiol. 2020;598:987–98. https://doi.org/10.1113/JP278788.

58. Zmigrod S, Zmigrod L, Hommel B. Transcranial direct current stimulation (tDCS) over the right dorsolateral prefrontal cortex affects stimulus conflict but not response conflict. Neuroscience. 2016;322:320–5. https://doi.org/10.1016/j.neuroscience.2016.02.046.

59. Cespón J, Hommel B, Korsch M, Galashan D. The neurocognitive underpinnings of the Simon effect: an integrative review of current research. Cogn Affect Behav Neurosci. 2020;20:1133–72. https://doi.org/10.3758/s13415-020-00836-y.

60. Salat DH, Buckner RL, Snyder AZ, Greve DN, Desikan RSR, Busa E, Morris JC, Dale AM, Fischl B. Thinning of the cerebral cortex in aging. Cereb Cortex. 2004;14:721–30. https://doi.org/10.1093/cercor/bhh032.

61. Raz N, Gunning FM, Head D, Dupuis JH, McQuain J, Briggs SD, Loken WJ, Thornton AE, Acker JD. Selective aging of the human cerebral cortex observed in vivo: differential vulnerability of the prefrontal gray matter. Cereb Cortex. 1997;7:268–82. https://doi.org/10.1093/cercor/7.3.268.

62. Raz N, Gunning-Dixon F, Head D, Rodrigue KM, Williamson A, Acker JD. Aging, sexual dimorphism, and hemispheric asymmetry of the cerebral cortex: replicability of regional differences in volume. Neurobiol Aging. 2004;25:377–96. https://doi.org/10.1016/S0197-4580(03)00118-0.

63. Good CD, Johnsrude IS, Ashburner J, Henson RNA, Friston KJ, Frackowiak RSJ. A voxel-based morphometric study of ageing in 465 normal adult human brains. Neuroimage. 2001;14:21–36. https://doi.org/10.1006/nimg.2001.0786.

64. Resnick SM, Pham DL, Kraut MA, Zonderman AB, Davatzikos C. Longitudinal magnetic resonance imaging studies of older adults: a shrinking brain. J Neurosci. 2003;23:3295–301. https://doi.org/10.1523/JNEUROSCI.23-08-03295.2003.

65. Koen JD, Rugg MD. Neural dedifferentiation in the aging brain. Trends Cogn Sci. 2019;23:547–59.

66. Li S-C, Lindenberger U, Frensch PA. Unifying cognitive aging: from neuromodulation to representation to cognition. Neurocomputing. 2000;32–33:879–90. https://doi.org/10.1016/S0925-2312(00)00256-3.

67. Li S-C, Rieckmann A. Neuromodulation and aging: implications of aging neuronal gain control on cognition. Curr Opin Neurobiol. 2014;29:148–58.

68. Mather M, Harley CW. The locus coeruleus: essential for maintaining cognitive function and the aging brain. Trends Cogn Sci. 2016;20:214–26. https://doi.org/10.1016/j.tics.2016.01.001.

69. Ren P, Anderson AJ, McDermott K, Baran TM, Lin F (2019) Cognitive fatigue and cortical-striatal network in old age. Aging 11, 2312–2326. https://doi.org/10.18632/aging.101915

70. Salthouse TA. The processing-speed theory of adult age differences in cognition. Psychol Rev. 1996;103:403.

71. Hillary FG, Genova HM, Chiaravalloti ND, Rypma B, DeLuca J. Prefrontal modulation of working memory performance in brain injury and disease. Hum Brain Mapp. 2006;27:837–47. https://doi.org/10.1002/hbm.20226.

72. Hull C (2020) Prediction signals in the cerebellum: beyond supervised motor learning. eLife 9, e54073. https://doi.org/10.7554/eLife.54073

73. Manto M, Bower JM, Conforto AB, Delgado-García JM, da Guarda SNF, Gerwig M, Habas C, Hagura N, Ivry RB, Mariën P, Molinari M, Naito E, Nowak DA, Ben Taib NO, Pelisson D, Tesche CD, Tilikete C, Timmann D. Consensus Paper: Roles of the cerebellum in motor control—the diversity of ideas on cerebellar involvement in movement. Cerebellum Lond Engl. 2012;11:457–87. https://doi.org/10.1007/s12311-011-0331-9.

74. Hirose S, Jimura K, Kunimatsu A, Abe O, Ohtomo K, Miyashita Y, Konishi S. Changes in cerebro-cerebellar interaction during response inhibition after performance improvement. Neuroimage. 2014;99:142–8. https://doi.org/10.1016/j.neuroimage.2014.05.007.

75. Galea JM, Jayaram G, Ajagbe L, Celnik P. Modulation of cerebellar excitability by polarity-specific noninvasive direct current stimulation. J Neurosci. 2009;29:9115–22. https://doi.org/10.1523/JNEUROSCI.2184-09.2009.

76. Mannarelli D, Pauletti C, Petritis A, Delle Chiaie R, Currà A, Trompetto C, Fattapposta F. Effects of cerebellar tDCS on inhibitory control: evidence from a go/nogo task. The Cerebellum. 2020;19:788–98. https://doi.org/10.1007/s12311-020-01165-z.

77. Andersen BB, Gundersen HJG, Pakkenberg B. Aging of the human cerebellum: a stereological study. J Comp Neurol. 2003;466:356–65. https://doi.org/10.1002/cne.10884.

78. Childs R, Gamage R, Münch G, Gyengesi E. The effect of aging and chronic microglia activation on the morphology and numbers of the cerebellar Purkinje cells. Neurosci Lett. 2021;751:135807. https://doi.org/10.1016/j.neulet.2021.135807.

79. Erb CD, Germine L, Hartshorne JK (2023) Cognitive control across the lifespan: congruency effects reveal divergent developmental trajectories. J Exp Psychol Gen

80. Little S, Bonaiuto J, Barnes G, Bestmann S. Human motor cortical beta bursts relate to movement planning and response errors. PLoS Biol. 2019;17:e3000479. https://doi.org/10.1371/journal.pbio.3000479.

81. Brady B, Power L, Bardouille T. Age-related trends in neuromagnetic transient beta burst characteristics during a sensorimotor task and rest in the Cam-CAN open-access dataset. Neuroimage. 2020;222:117245. https://doi.org/10.1016/j.neuroimage.2020.117245.

82. Wilson TW, Heinrichs-Graham E, Becker KM. Circadian modulation of motor-related beta oscillatory responses. Neuroimage. 2014;102:531–9. https://doi.org/10.1016/j.neuroimage.2014.08.013.